Received: 16 May 2023 | Revised: 3 April 2024 | Accepted: 16 April 2024

DOI: 10.1096/fba.2023-00051

RESEARCH ARTICLE

FASEB BioAdvances WILEY

The effects of oxidative stress and intracellular calcium on mitochondrial permeability transition pore formation in equine spermatozoa

Zamira Gibb[1] | **Robert J. Aitken**[1] | **Alecia R. Sheridan**[1] | **Brandan Holt**[2] | **Stephanie Waugh**[1] | **Aleona Swegen**[1]

[1]School of Environmental and Life Sciences, College of Engineering, Science and Environment, The University of Newcastle, Callaghan, New South Wales, Australia

[2]Faculty of Health, School of Biomedical Sciences, Queensland University of Technology, Brisbane, Queensland, Australia

Correspondence
Zamira Gibb, LS4.45 School of Environmental and Life Sciences, College of Engineering, Science and Environment, The University of Newcastle, Callaghan, NSW 2308, Australia.
Email: zamira.gibb@newcastle.edu.au

Funding information
Australian Research Council, Grant/Award Number: DE180100894 and FT220100557

Abstract

The in vitro storage of stallion spermatozoa for use in artificial insemination leads to oxidative stress and imbalances in calcium homeostasis that trigger the formation of the mitochondrial permeability transition pore (mPTP), resulting in premature cell death. However, little is understood about the dynamics and the role of mPTP formation in mammalian spermatozoa. Here, we identify an important role for mPTP in stallion sperm Ca^{2+} homeostasis. We show that stallion spermatozoa do not exhibit "classical" features of mPTP; specifically, they are resistant to cyclosporin A-mediated inhibition of mPTP formation, and they do not require exogenous Ca^{2+} to form the mPTP. However, chelation of endogenous Ca^{2+} prevented mPTP formation, indicating a role for intracellular Ca^{2+} in this process. Furthermore, our findings suggest that this cell type can mobilize intracellular Ca^{2+} stores to form the mPTP in response to low Ca^{2+} environments and that under oxidative stress conditions, mPTP formation preceded a measurable increase in intracellular Ca^{2+}, and vice versa. Contrary to previous work that identified mitochondrial membrane potential (MMP) as a proxy for mPTP formation, here we show that a loss of MMP can occur independently of mPTP formation, and thus MMP is not an appropriate proxy for the detection of mPTP formation. In conclusion, the mPTP plays a crucial role in maintaining Ca^{2+} and reactive oxygen species homeostasis in stallion spermatozoa, serving as an important regulatory mechanism for normal sperm function, thereby contraindicating the in vitro pharmacological inhibition of mPTP formation to enhance sperm longevity.

Abbreviations: AA, arachidonic acid; ACEC, Animal Care and Ethics Committee; AFU, arbitrary fluorescence units; ANOVA, analysis of variance; BAPTA-AM, 1,2-bis(2-aminophenoxy)ethane-*N*,*N*,*N*′,*N*′-tetraacetic acid tetrakis(acetoxymethyl ester); BWW, Biggers, Whitten, and Whittingham medium; C-AM, calcein AM/$CoCl_2$ assay; C-AM-G, calcein AM Green/$CoCl_2$ assay; C-AM-V, calcein AM Violet/$CoCl_2$ assay; CCCP, carbonyl cyanide *m*-chlorophenylhydrazone; CsA, cyclosporin A; CyPD, cyclophilin D; ETC, electron transport chain; HEPES, 2-[4-(2-hydroxyethyl) piperazin-1-yl]ethanesulfonic acid; JC-1, 5,5′,6,6′-tetrachloro-1,1′,3,3′-tetraethylimidacarbocyanine iodide; LDFR, LIVE/DEAD Fixable Far Red Stain; LDV, LIVE/DEAD Fixable Violet Stain; MMP, mitochondrial membrane potential; mPTP, mitochondrial permeability transition pore; MSR, MitoSOX™ Red stain; NOX, nicotinamide adenine dinucleotide phosphate (NADPH) oxidase; PI, propidium iodide; ROS, reactive oxygen species.

KEYWORDS
horse, JC-1, mitochondrial permeability transition pore, oxidative stress, spermatozoa

1 | INTRODUCTION

The loss of sperm functionality and fertility in vitro is primarily attributed to the downstream effects of reactive oxygen species (ROS)-induced oxidative stress.[1,2] Spermatozoa are generally cooled or cryopreserved for storage, with a mind to restrict metabolism and thereby reduce the production of mitochondria-derived ROS during storage. However, as spermatozoa cool, the lipid membrane architecture is altered, resulting in a reduction in membrane fluidity which then leads to the dysregulated movement of ions, such as calcium, across the plasma membrane and a concomitant loss of sperm function.[3,4]

Calcium-mediated signaling pathways are implicated in almost every cellular function, and the spermatozoon is no exception. Calcium ions are required for all stages of sperm maturation, from the acquisition of motility, through to capacitation and the acrosome reaction, along with the act of fertilization and oocyte activation.[5] However, when calcium homeostasis is perturbed through processes such as chilling,[4] or intracellular calcium levels are artificially boosted by exposure to agents such as calcium ionophores, the result is a loss of sperm motility and viability,[6] which may be explained in part by the formation of the mitochondrial permeability transition pore (mPTP).[4] The phenomenon of mPTP formation is associated with the sudden onset of mitochondrial inner-membrane unselective 'leakiness' and has been observed in numerous cell types and organisms. The mPTP is a regulated channel that renders the inner mitochondrial membrane permeable to ions and solutes of less than 1500 Da in size, and while transient pore formation is believed to be associated with normal calcium and ROS homeostasis, prolonged mPTP formation leads to mitochondrial matrix swelling, the uncoupling of oxidative phosphorylation and eventually, apoptosis or necrosis.[7]

The mPTP is enigmatic, and the sperm mPTP is even more so. While the structure of the mPTP is yet to be ascertained, a number of hypothetical structures have been postulated. These structures have implicated adenine nucleotide translocase,[8] mitochondrial phosphate carriers,[9] the formation of ATP synthase dimers,[10] the loss of ATP synthase dimerization,[11] and the ATP synthase c subunit.[11] A comprehensive review of the history and evolution of mPTP research over the last 40 years has been published by Baines and Gutierrez-Aguilar.[12] Despite the longstanding debate about mPTP structure, particular features that are generally agreed upon are an absolute specificity for Ca^{2+} and inhibition by cyclosporin A (CsA), a cyclophilin D (CyPD) inhibitor, the use of which has been shown to desensitize the mPTP to the effects of elevated calcium, at least in the case of somatic cells.[13,14]

The universally accepted assay for measuring mPTP formation in somatic cells is the calcein AM/$CoCl_2$ (C-AM) assay, although the measurement of mitochondrial membrane potential (MMP) using the 5,5′,6,6′-tetrachloro-1,1′,3,3′-tetraethylimidacarbocyanine iodide (JC-1) probe has often been utilized as an indirect measure of mPTP formation.[15–17] Use of the calcein AM/$CoCl_2$ assay was first described by Petronilli et al.[18] who were seeking a more direct method to quantify mPTP formation than the aforementioned downstream markers. Given that mPTP formation is known to be sensitive to CsA inhibition, and indeed, the C-AM assay corroborates this phenomenon in somatic cells, it is somewhat confounding that according to the C-AM assay, CsA does not inhibit mPTP formation in mammalian spermatozoa,[19] suggesting that mammalian sperm mitochondria do not undergo mPTP formation in the classical sense. Nonetheless, several studies have recently emerged in which mPTP formation has been confirmed in the spermatozoa of several species, including the horse.[17,19–23] A limitation of many of these studies has been the use of downstream markers of mPTP formation, such as caspase activation, oxidative stress, loss of viability and/or motility, and mitochondrial membrane depolarisation, to quantify mPTP formation following various treatments. However, these events may be initiated by any number of insults and cannot definitively be attributed to mPTP formation in the absence of a C-AM assay.

The aim of this study was therefore to characterize the events surrounding mPTP formation in stallion spermatozoa, a cell type that is known to be heavily dependent upon mitochondrial respiration for the production of energy.[24,25] We hypothesized that the stallion sperm mPTP plays a vital role in the maintenance of calcium and ROS homeostasis and that the C-AM assay will provide a sensitive measure of mPTP formation.

2 | MATERIALS AND METHODS

2.1 | Materials

Unless otherwise stated, all chemicals were purchased from Sigma-Aldrich. A modified Biggers, Whitten, and Whittingham medium (BWW[26]) containing 95 mM NaCl, 4.7 mM KCl, 1.7 mM $CaCl_2 \cdot 2H_2O$, 1.2 mM KH_2PO_4, 1.2 mM

$MgSO_4 \cdot 7H_2O$, 25 mM $NaHCO_3$, 5.6 mM D-Glucose, 275 μM $C_3H_3NaO_3$, 3.7 μL/mL 60% sodium lactate syrup, 50 U/mL penicillin, 50 μg/mL streptomycin, 20 mM 2-[4-(2-hydroxyethyl) piperazin-1-yl]ethanesulfonic acid (HEPES), and 0.1% (w/v) polyvinyl alcohol, with an osmolarity of 310 mOsm/kg, was utilized throughout this study. All semen collection equipment and EquiPlus extender were purchased from Minitube Australia (Ballarat, VIC, Australia).

2.2 | Preparation of stallion spermatozoa

For all proceeding experiments, spermatozoa were collected and processed according to the following protocol. Institutional and New South Wales State Government ethical approval was secured for the use of animal material in this study (ACEC number A2011-122). Experiments were based on multiple ejaculates from five normozoospermic Shetland and Miniature crossbred pony stallions (between 2 and 15 years of age) of proven fertility, held on institutionally approved premises. The stallions had access to native pasture 24 h a day and were supplementary fed with grass hay, Lucerne chaff, canola oil, salt, and minerals once daily. Semen was collected using a pony-sized Missouri artificial vagina with an inline semen filter, and the ejaculate was immediately diluted (2:1; extender:semen) with EquiPlus liquid extender (Minitube; Ballarat). Equipment and extender were maintained at 37°C for the duration of semen collection and dilution. Extended semen was allowed to cool to RT, and high-quality spermatozoa were isolated using density gradient centrifugation. Briefly, 6 mL of extended semen was overlaid on 3 mL of EquiPure (Tek-Event Pty Ltd, Round Corner, NSW, Australia) in a 15 mL conical centrifuge tube (Falcon; Livingstone, Mascot, NSW, Australia). Gradients were centrifuged at 400 *g* for 20 min, the supernatant removed, and the resulting pellet (containing high-quality equine spermatozoa) was resuspended in BWW to a final concentration of 20×10^6 spermatozoa/mL for use in experiments. Washed spermatozoa were stored under aerobic conditions for all following procedures.

2.3 | Flow cytometry

All flow cytometry was performed using a FACSCanto II Cell Analyzer (BD Bioscience, NJ, USA) with three lasers: blue (488 nm air-cooled, 20 mW solid state), red (633 nm, 17 mW HeNe), and violet (405 nm, 30 mW solid state). Emission measurements were made using 450/50 bandpass (violet/BV421), 530/30 bandpass (green/Alexa Fluor 488), 585/42 band pass (red/PE), and >670 long pass (far red/APC) filters. Debris were gated out using a forward scatter/side scatter dot plot, and a minimum of 10,000 cells were analyzed per sample. All data were analyzed using FACSDiva software (BD Bioscience).

2.4 | Flow cytometric assays

2.4.1 | mPTP formation (calcein AM green/$CoCl_2$; C-AM-G assay)

The C-AM probe is membrane permeable and nonfluorescent in its esterified state, but once loaded into the cell, cytosolic esterases de-esterify the molecule, making it highly fluorescent and membrane impermeable. In order to restrict the fluorescence signal to the mitochondria, $CoCl_2$ is added after C-AM to selectively quench the cytosolic calcein signal, with any subsequent loss of fluorescence of the membrane-impermeable probe being attributable to loss of the probe via the mPTP. As such, low C-AM fluorescence indicates mPTP formation.

Following treatment, 100 μL of sperm suspension were incubated with 0.1 μM C-AM green (C-AM-G; ThermoFisher) and 0.4 mM $CoCl_2$ (added at least 2 min after C-AM-G). Sperm suspensions were then incubated for 15 min at 37°C in the dark, after which they were centrifuged at 500 *g* for 3 min, supernatant removed, and sperm pellet re-suspended for flow cytometric analysis in 400 μL BWW containing 7.5 μM propidium iodide (PI) as a viability stain. Single stain controls were utilized to set quadrant gates: for the C-AM-G negative control, ionomycin (1 μM final concentration) was added following the addition of C-AM-G, but prior to incubation; a PI-positive control was generated by repeat snap freeze-thawing of the sperm suspension prior to resuspension in BWW/PI solution. Ionomycin, a Ca^{2+} ionophore, is used as a negative control as it allows entry of excess Ca^{2+} into the cells, which triggers mitochondrial pore activation and subsequent loss of mitochondrial calcein fluorescence. Green (Alexa Fluor 488 channel) and red fluorescence (PE channel) events were collected, with high red cells being nonviable (PI bright) and low green cells (C-AM-G dim) having formed the mPTP. The median C-AM-G fluorescence signal from viable cells was also collected, with either the percent of high C-AM-G cells or the median C-AM-G fluorescence (arbitrary fluorescence units [AFU]) being reported, depending on the experiment.

2.4.2 | Mitochondrial ROS (MitoSOX™ Red) assay

The MitoSOX Red (MSR) reagent is membrane permeable and by virtue of its charge can specifically target the mitochondria.

Under conditions of high mitochondrial ROS, the reagent is oxidized by superoxide ($O_2^{\bullet-}$) and becomes highly fluorescent, allowing for a direct measurement of mitochondrial $O_2^{\bullet-}$ production. To run the MSR assay, 100 µL of sperm suspension was incubated for 15 min at 37°C with 2 µM MSR stain (Molecular Probes, Australia) and 5 nM SYTOX Green (SyG; Molecular Probes) viability stain. Staining controls included: a positive dead control: 100 µL of sperm suspension was repeatedly snap frozen/thawed and incubated for 15 min at 37°C with 5 nM SyG viability stain only; and an MSR positive control in which 100 µL of sperm was incubated for 15 min with 100 µM arachidonic acid (AA) and 2 µM MSR stain only. The spermatozoa were then centrifuged at 500*g* for 3 min; supernatant was removed, and pellets were resuspended in 400 µL BWW for flow cytometric analysis. In non-viable cells, MSR (an ethidium-based fluorophore) can access and bind to the DNA, and as such, nonviable sperm are always positive for MSR stain; however, this is an artifact, as dead cells cannot produce superoxide. For this reason, only viable cell data were used for statistical analyses of MSR assays.

2.4.3 | MMP (JC-1 assay)

The JC-1 stain is accumulated in the mitochondria in a potential-dependent manner. When in monomeric form, as is the case when MMP is low, the stain emits a green fluorescence (529 nm). When MMP is high, JC-1 accumulates in the mitochondria and forms aggregates, which emit a red fluorescence (590 nm).

In this study, 100 µL aliquots of spermatozoa were incubated with 2 µM JC-1 and 1:5000 LIVE/DEAD Fixable Far Red (LDFR; both from ThermoFisher) for 15 min at 37°C in the dark, after which they were centrifuged at 500*g* for 3 min; supernatant was removed, and pellets were resuspended in 400 µL BWW for flow cytometric analysis.

Staining controls included a JC-1 negative control: spermatozoa were incubated with 10 µM carbonyl cyanide *m*-chlorophenylhydrazone (CCCP) and 2 µM JC-1 only for 15 min at 37°C; and an LDFR positive control: spermatozoa were snap frozen in liquid nitrogen and then incubated for 15 min at 37°C with LDFR viability stain only. Only Live cells (LDFR dim) were gated into the JC-1 dot plot for analysis, and the CCCP negative control was used to set the gate between the high and low MMP populations.

2.4.4 | Intracellular calcium/mitochondrial ROS (Fluo-4 AM/MSR) dual stain assay

Fluo-4 AM is membrane permeable in its esterified state, but once loaded into the cell, cytosolic esterases de-esterify the molecule, making it membrane impermeable. Upon binding to Ca^{2+}, the fluorescence intensity of Fluo-4 AM increases more than 100-fold.

For the combined Fluo-4 AM/MSR assay, 1 mL of sperm suspension from each ejaculate was pre-loaded with 2 µM Fluo-4 AM (ThermoFisher) for 15 min at 37°C before being centrifuged and the sperm pellet re-suspended in an equal volume of BWW prior to dividing into aliquots for treatment. Following treatment, 100 µL aliquots of sperm suspension were simultaneously stained with 2 µM MSR, and 1:5000 LIVE/DEAD Violet (LDV; ThermoFisher) for 15 min at 37°C, after which they were centrifuged at 500*g* for 3 min; supernatant was removed, and pellets were resuspended in 400 µL BWW for flow cytometric analysis. Live spermatozoa (LDV dim; BV421 channel) were gated into a second dot plot in which MSR (PE channel) and Fluo-4 (Alexa Fluor 488 channel) brightness were determined. Single stain positive controls were generated in order to set the regions and quadrants for determination of MSR, Fluo-4, and LDV brightness. For MSR the positive control was 100 µM AA (added just prior to MSR stain), for Fluo-4 AM the positive control was 1 µM ionomycin (added after Fluo-4 AM pre-loading), and for LDV an aliquot of sperm suspension was repeatedly snap frozen and thawed prior to addition of LDV stain.

2.4.5 | Mitochondrial ROS/mPTP formation (MSR/C-AM-G) dual stain assay

For the combined MSR/mPTP assay, 100 µL aliquots of sperm suspension were simultaneously stained with 0.1 µM C-AM-G, 2 µM MSR, and 1:5000 LDV, after which 0.4 mM $CoCl_2$ was added as per mPTP assay (Section 2.4.1), sperm suspensions were incubated for 15 min at 37°C in the dark, after which they were centrifuged at 500*g* for 3 min; supernatant was removed, and pellets were resuspended in 400 µL BWW for flow cytometric analysis. Live spermatozoa (LDV dim; BV421 channel) were gated into a second dot plot in which MSR (PE channel) and C-AM-G (Alexa Fluor 488 channel) brightness were determined. Single stain controls were generated in order to set the regions and quadrants for determination of MSR, C-AM-G, and LDV brightness. For MSR, the positive control was 100 µM AA (added just prior to MSR stain), for C-AM-G, the negative control was 1 µM ionomycin (added just prior to C-AM-G stain addition), and for LDV, an aliquot of sperm suspension was repeatedly snap frozen and thawed prior to addition of LDV stain.

2.4.6 | MMP/mPTP formation (JC-1/C-AM-V) assay

For the combined MMP/mPTP assay, 100 µL aliquots of sperm suspension were simultaneously stained with

0.1 μM calcein AM Violet (C-AM-V), 2 μM JC-1, and 1:5000 LDFR, after which 0.4 mM $CoCl_2$ was added as per mPTP assay (Section 2.4.1) to quench the cytosolic calcein signal. Sperm suspensions were incubated for 15 min at 37°C in the dark, after which they were centrifuged at 500 *g* for 3 min; supernatant was removed, and pellets were resuspended in 400 μL BWW for flow cytometric analysis. Live spermatozoa (LDFR dim; Alexa Fluor 647 channel) were gated into a second dot plot in which high and low MMP sperm populations were gated using a PE/Alexa Fluor 488 channel dot plot. These high and low MMP populations were each gated into histogram plots to determine C-AM-V brightness (BV421 channel). Single stain controls were generated in order to set the regions and quadrants for determination of JC-1, C-AM-V, and LDFR brightness. For JC-1, the negative control was 10 μM CCCP (added prior to JC-1 as per Section 2.4.3), for C-AM-V, the negative control was 1 μM ionomycin (added after C-AM-V stain addition), and for LDFR, an aliquot of sperm suspension was repeatedly snap frozen and thawed prior to addition of LDFR stain. Representative dot plots showing gating and staining controls are shown in Figure 1.

2.5 | Statistical analyses

Data were analyzed using IBM SPSS Statistics 27 software. Data were checked for normal distribution of residuals (Shapiro–Wilk test), and if residuals were normally distributed and Levene's test revealed homogeneity of variance, a one-way analysis of variance (ANOVA) was conducted to determine treatment effects. If Levene's test revealed nonhomogeneity of variance, the Welch test statistic was used to identify significant treatment effects. If ANOVA or the Welch test statistic revealed a significant treatment

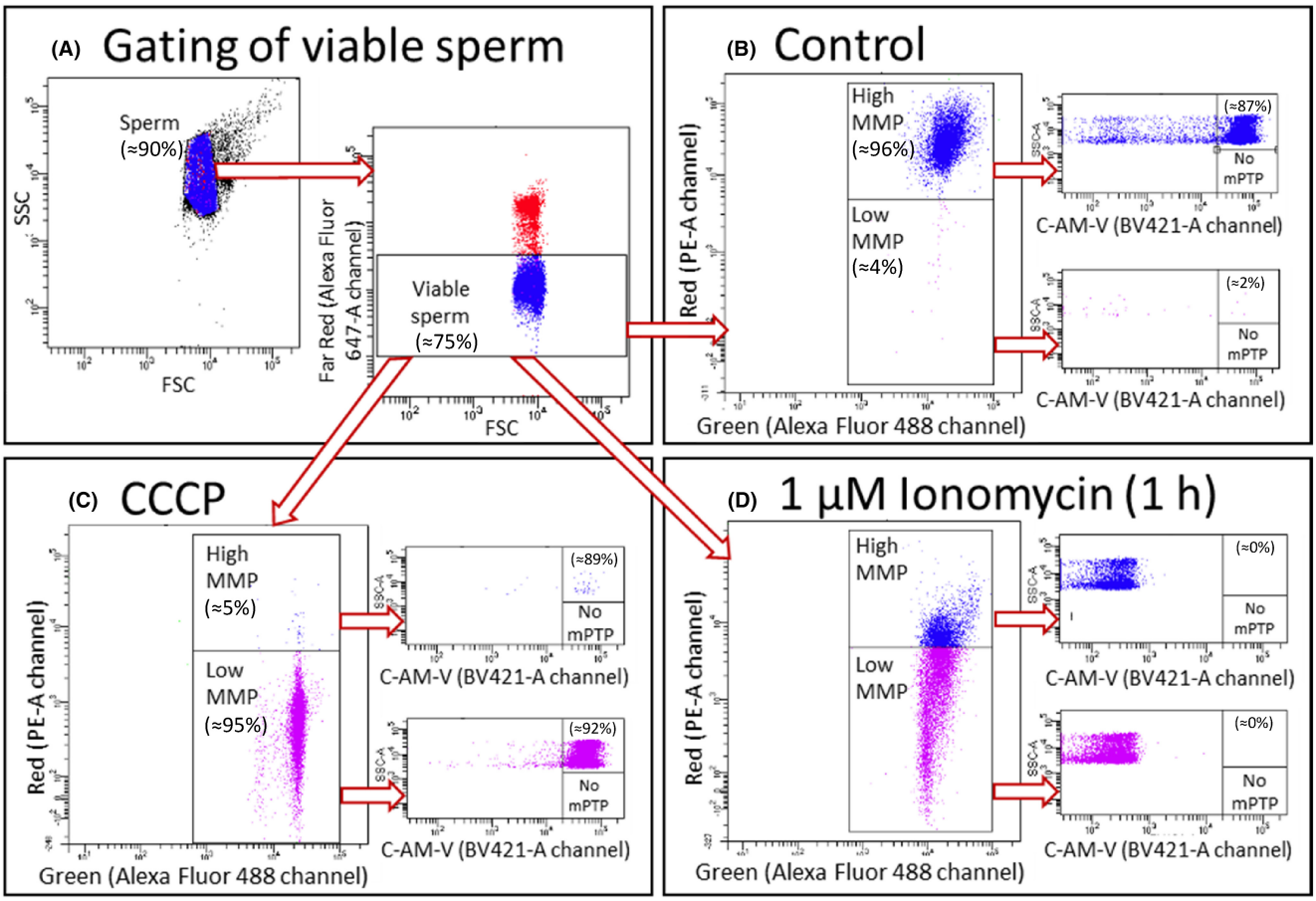

FIGURE 1 Representative flow cytometric dot plots of triple-stained (Far Red LIVE/DEAD, JC-1, and calcein AM Violet [C-AM-V]) stallion spermatozoa. (A) Spermatozoa were gated from debris (using a forward scatter; FSC/side-scatter; SSC dot plot) into a second plot to gate viable spermatozoa (Far Red LIVE/DEAD dim) into subsequent JC-1 plots to determine mitochondrial membrane potential (MMP). (B–D) Representative flow cytometric dot plots showing the control treatment (B), CCCP negative control for JC-1 gating (C), and 1 μM ionomycin treatment at 1 h (D). From the JC-1 plots, high or low MMP spermatozoa were gated into C-AM-V/SSC plots to determine the mPTP formation status of these populations. Created using Biorender.com. CCCP, carbonyl cyanide *m*-chlorophenylhydrazone; mPTP, mitochondrial permeability transition pore.

effect, a Dunnets test was used to compare treatments to the control. If residuals were not normally distributed, a nonparametric Kruskal–Wallis test was utilized to determine treatment effects. For these nonparametric data, comparisons to the control were conducted using pairwise comparisons with Bonferroni corrections. For each test, a p-value of ≤0.05 indicated a significant difference. All raw data that support the findings of this study are available as Supporting Information for this article.

3 | RESULTS

3.1 | Experiment 1. MMP loss and mPTP formation do not occur simultaneously

To determine the effect of various doses of ionomycin on mPTP formation and MMP, isolated spermatozoa from three individual stallions were exposed to 0 (control), 0.25, 0.5, 1, and 4 μM ionomycin during JC-1/C-AM-V/LDFR staining (15 min). The MMP/mPTP assay was run as described in Section 2.4.6. To determine the effect of prolonged mPTP formation on MMP, spermatozoa were exposed to 0 (control) or 1 μM ionomycin for 0, 1, 2, and 4 h, after which the mPTP/MMP assay was performed.

Although there was a highly significant treatment effect of ionomycin dose on mPTP ($p \leq 0.001$), there was no dose-dependent effect of 15 min ionomycin treatment on MMP. At all ionomycin doses, mPTP formation was highly significant compared with the control (control: 86.7 ± 7.9% bright C-AM-V vs. 0 ± 0% bright C-AM-V spermatozoa for all ionomycin doses; all $p \leq 0.001$; Figure 2A).

When spermatozoa were incubated with 1 μM ionomycin over 3 h, there was a significant effect of incubation time on MMP ($p \leq 0.001$). Compared with $t = 0$ h (91.2 ± 3.8% high MMP), the MMP of ionomycin-treated spermatozoa declined significantly by 1 h (43.5 ± 12.5% high MMP; $p \leq 0.05$), a difference which became highly significant by 2 and 3 h (21.3 ± 15.3% and 5.4 ± 2.8% high MMP respectively; both $p \leq 0.001$). There was no effect of incubation time on mPTP formation of control or ionomycin-treated spermatozoa nor was there an effect of incubation time on the MMP of control spermatozoa (Figure 2B).

3.2 | Experiment 2. Stallion sperm mPTP formation in response to increased intracellular calcium cannot be inhibited by CsA

To determine the minimum ionomycin dose required to elicit mPTP formation, stallion ejaculates ($n = 9$) were collected, and a dose response was conducted using 0 (control), 5, 10, 20, 40, 80, and 160 μM ionomycin during C-AM-G staining

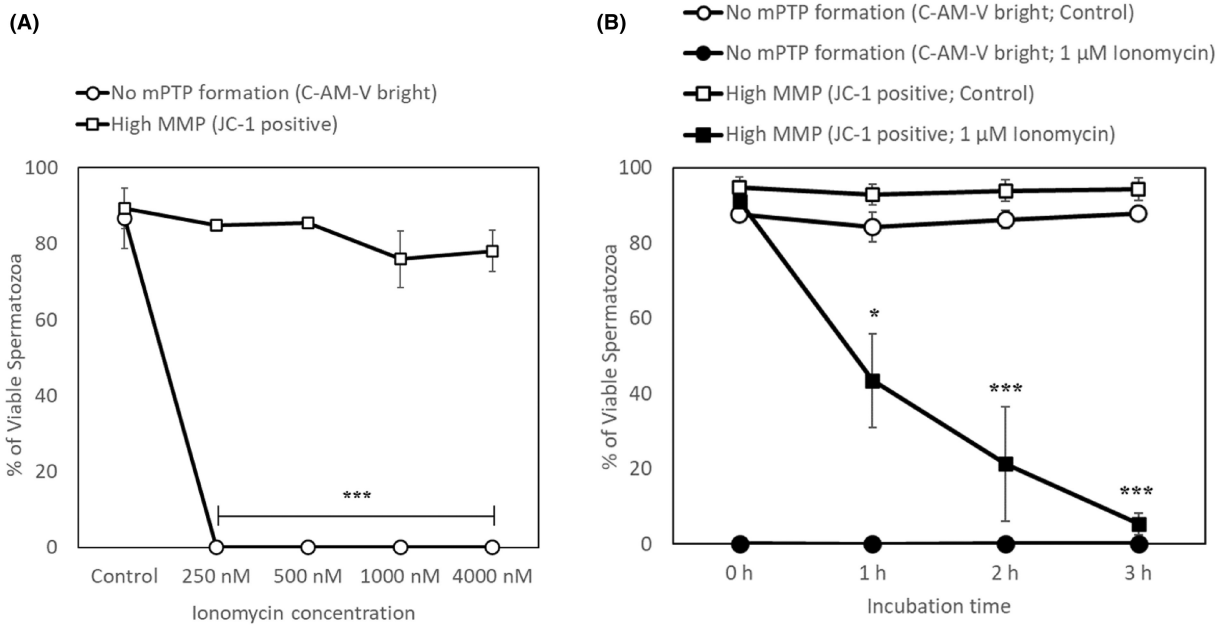

FIGURE 2 Mitochondrial permeability transition pore (mPTP) formation in stallion spermatozoa is not immediately accompanied by a loss of mitochondrial membrane potential (MMP). (A) Percentage of C-AM-V bright (no mPTP formation) and high MMP of stallion spermatozoa exposed to various ionomycin doses. (B) Percentage of C-AM-V bright (no mPTP formation) and high MMP of stallion spermatozoa exposed to 1 μM ionomycin for 0, 1, 2, and 3 h. $N = 3$ split ejaculates. Significant difference from the control (A) or $t = 0$ h (B) denoted by *$p \leq 0.05$ or ***$p \leq 0.001$. C-AM-V, calcein AM Violet.

after which the mPTP assay was conducted (Section 2.4.1). There was a significant effect of ionomycin treatment on mPTP formation ($p \leq 0.001$), with the C-AM-G signal being significantly lower than the control at all doses (control: 100 ± 16.4 AFU, 5 nM ionomycin: 44.3 ± 8.3 AFU, 10 nM ionomycin: 34.7 ± 7.6 AFU, 20 nM ionomycin: 20.8 ± 5.8 AFU, 40 nM ionomycin: 13.0 ± 3.5 AFU, 80 nM ionomycin: 5.8 ± 2.2 AFU, 160 nM ionomycin: 4.4 ± 1.9 AFU; all data normalized to the control; all $p \leq 0.001$; Figure 3A) indicating a calcium-dependent pore opening event.

To ascertain whether CsA could inhibit calcium (Ca^{2+})-induced mPTP formation, spermatozoa were incubated with 0, 5, 10, and 20 μM CsA for 30 min prior to the addition of 10 nM ionomycin during C-AM-G staining. A control sample (no CsA or ionomycin) was included. Following C-AM-G staining, sperm pellets were resuspended in BWW containing corresponding concentrations of CsA to ensure that any subsequent mPTP formation was not due to CsA removal, after which the mPTP assay was conducted (Section 2.4.1). Pretreatment with CsA did not inhibit mPTP formation at any dose, with all spermatozoa treated with 10 nM ionomycin—the IC_{50} dose identified in Figure 3A—having significantly lower C-AM-G fluorescence compared with the control ($p \leq 0.001$) irrespective of CsA dose (control: 100 ± 1.5 AFU, 10 nM ionomycin: 51.2 ± 6.1 AFU, 5 μM CsA + ionomycin: 47.6 ± 6.4 AFU, 10 μM CsA + ionomycin: 45.2 ± 6.7 AFU, 20 μM CsA + ionomycin: 43.1 ± 6.5 AFU; Figure 3B).

To ascertain whether exogenous Ca^{2+} is required for mPTP formation, isolated sperm suspensions ($n = 9$ ejaculates prepared as per Section 2.2) were divided into two aliquots which were washed twice through either normal BWW (control) or Ca^{2+}-free BWW (osmotically balanced with NaCl) to ensure complete removal of exogenous Ca^{2+} from the latter. Spermatozoa were then incubated at 37°C for 1 h, after which the mPTP assay was conducted (Section 2.4.1). Spermatozoa were maintained in either regular BWW (control) or Ca^{2+}-free BWW for the entire duration of the experiment and assay. Paradoxically, incubation of spermatozoa in Ca^{2+}-free BWW also induced highly significant mPTP formation compared with the control (Control: 100 ± 4.2 AFU, Ca^{2+}-free BWW: 0.88 ± 0.2 AFU, $p \leq 0.001$; Figure 3C). A representative flow cytometry dot plot showing the shift in C-AM-G fluorescence with Ca^{2+} removal is shown in Figure 3D.

3.3 | Experiment 3. The stallion sperm mPTP is implicated in Ca^{2+} homeostasis in a reversible manner

We hypothesized that the mPTP formation observed in the Ca^{2+}-free treatment (Figure 3C,D) was an attempt to re-establish Ca^{2+} homeostasis by facilitating rapid Ca^{2+} entry into the mitochondria via the mPTP. To investigate whether this mPTP formation was associated with Ca^{2+} homeostasis under conditions of hypocalcemia, spermatozoa were deprived of Ca^{2+} for 30 min, after which Ca^{2+} was reintroduced at 0%, 25% (0.425 mM), 50% (0.85 mM), or 100% (1.7 mM) of that of regular BWW for a further 30 min (whereby regular BWW medium represents the physiological concentration of Ca^{2+} as found in the mammalian oviduct).[26] A BWW control (incubated for a total of 1 h) was also included. All samples were incubated at 37°C for the duration of the experiment, after which the mPTP assay was conducted (Section 2.4.1).

There was a significant treatment effect of Ca^{2+} deprivation and replacement on mPTP formation ($p \leq 0.001$). As in Experiment 2, incubation of spermatozoa in Ca^{2+}-free BWW resulted in mPTP formation (Control: 100 ± 9.2 AFU, Ca^{2+}-free BWW: 9.3 ± 1.0 AFU, $p \leq 0.001$), which was reversible with the replacement of Ca^{2+} in a dose-dependent manner. When Ca^{2+} was replaced at 0.425 mM, which is 25% of the "normal" BWW concentration (1.7 mM) for 30 min following Ca^{2+} deprivation, C-AM-G fluorescence increased to 36.3 ± 8.3 AFU ($p \leq 0.001$ compared with the control); when Ca^{2+} was replaced at 0.85 mM, which is 50% of the "normal" BWW concentration for 30 min following Ca^{2+} deprivation, C-AM-G fluorescence increased to 62.0 ± 10.7 AFU ($p \leq 0.01$ compared with the control); and when Ca^{2+} was replaced at the "normal" BWW concentration for 30 min following Ca^{2+}-deprivation, C-AM-G fluorescence increased to 92.3 ± 9.1 AFU which was not different to the control (Figure 4A). Figure 4B depicts a representative flow cytometric histogram showing the effects of Ca^{2+} deprivation and replacement on mPTP formation measured by C-AM-G staining intensity of viable spermatozoa.

3.4 | Experiment 4. The stallion sperm mPTP forms under physiological oxidative stress conditions

Oxidative stress was induced using either exogenous (H_2O_2) or endogenous (stimulated by AA)[27,28] sources of ROS. Spermatozoa were incubated with various doses of H_2O_2 (0, 0.25, 0.5, 1, 2, and 5 mM) and AA (0, 2.5, 5, 10, 20, and 40 μM) for 45 min at 37°C prior to the 15 min mPTP assay being conducted (Section 2.4.1), meaning that they were exposed to oxidative stressors for a total of 1 h.

Both exogenous (H_2O_2) and endogenous (stimulation of mitochondrial ROS production using AA) sources of oxidative stress caused mPTP formation. ANOVA

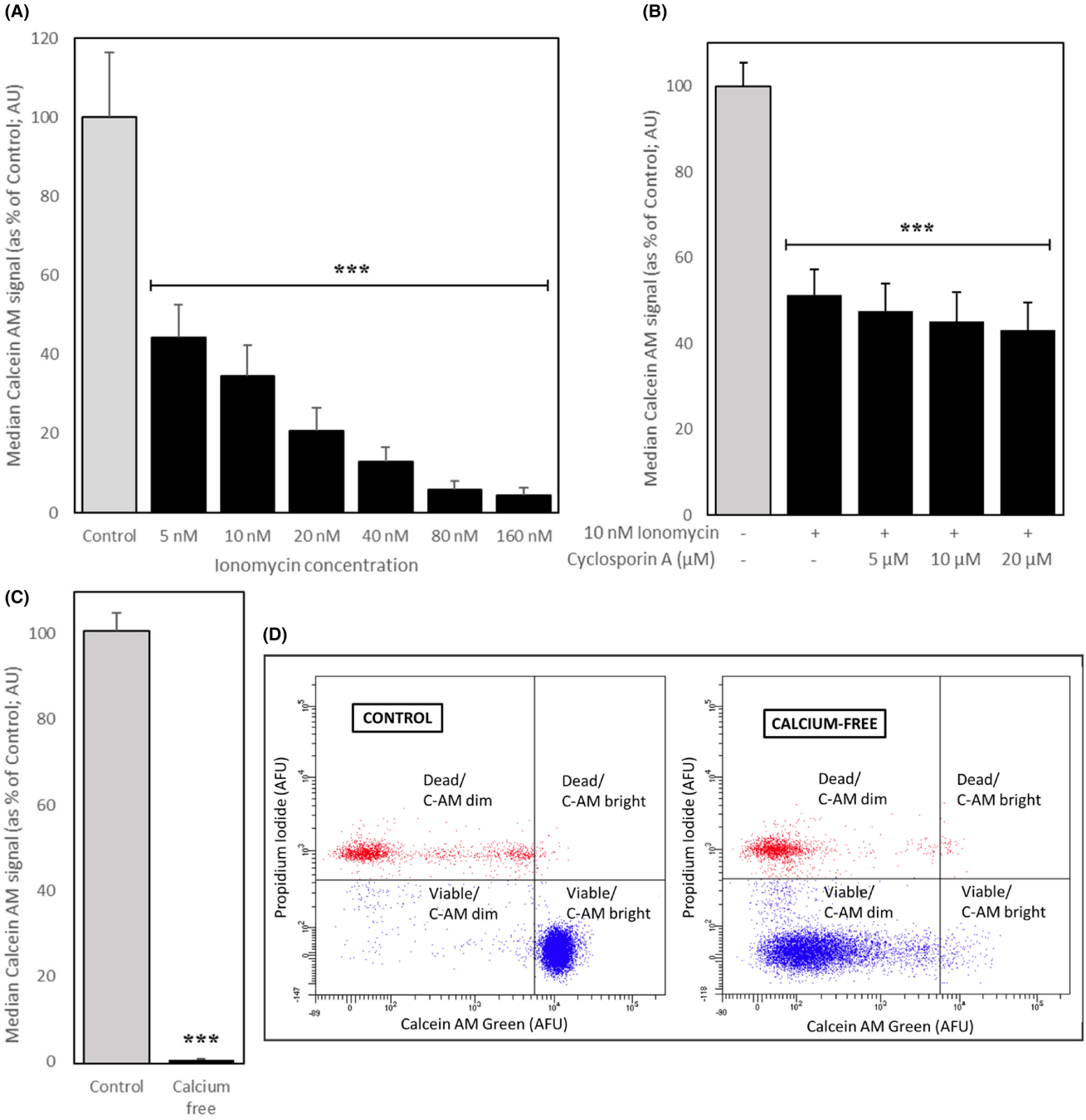

FIGURE 3 Stallion spermatozoa do not exhibit classical mitochondrial permeability transition pore (mPTP) formation. The stallion sperm mPTP formed in response to ionomycin-induced calcium (Ca^{2+}) influx (A), but the mPTP could not be inhibited by pretreatment with cyclosporin A (B). The stallion sperm mPTP is not dependent on an exogenous source of Ca^{2+}; complete mPTP formation occurs in a Ca^{2+}-free medium without any additional stimuli [(C) mean of the median calcein AM signal, (D) representative flow cytometric dot plots]. $N = 9$ split ejaculates. Significant difference from the control (gray bar) denoted by ***$p \leq 0.001$.

revealed a treatment effect of both H_2O_2 and AA on C-AM-G fluorescence intensity (both $p \leq 0.001$). All H_2O_2 doses produced lower C-AM-G signals compared with the control (control: 100 ± 3.7 AFU vs. 0.25 mM: 80.4 ± 4.5 AFU, $p \leq 0.01$; 0.5 mM: 75.5 ± 6.2 AFU, $p \leq 0.001$; 1 mM: 65.6 ± 3.5 AFU, $p \leq 0.001$; 2 mM: 56.8 ± 3.2 AFU, $p \leq 0.001$; 5 mM: 48.9 ± 4.1 AFU, $p \leq 0.001$; Figure 5A) indicating a redox-regulated opening of the mPTP. While there was no significant difference between the control and the lowest dose of AA (2.5 μM) on C-AM-G fluorescence (100 ± 13.0 AFU vs. 88.2 ± 13.4 AFU, respectively), all doses of AA at or above 5 μM produced lower C-AM-G fluorescence signals than the control (5 μM: 78.2 ± 13.3 AFU, $p \leq 0.05$; 10 μM: 51.2 ± 9.2 AFU, $p \leq 0.001$; 20 μM:

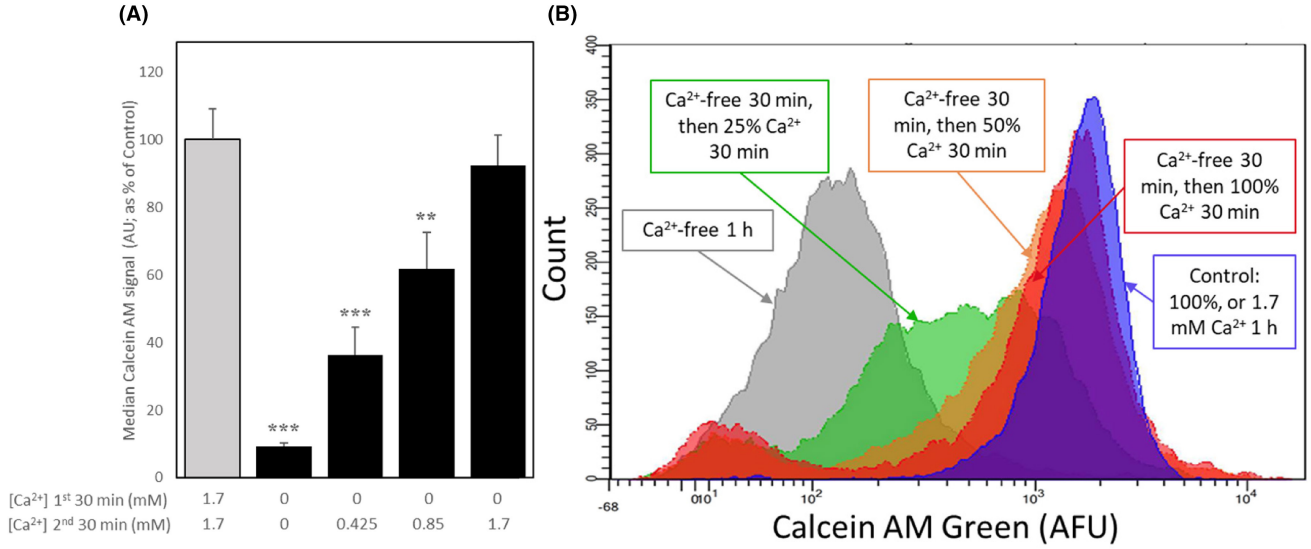

FIGURE 4 The stallion sperm mitochondrial permeability transition pore (mPTP) is responsible for maintaining calcium (Ca^{2+}) homeostasis-assessed using calcein AM Green (C-AM-G) staining and flow cytometry. (A) Mean ± SEM of the median C-AM-G signals from spermatozoa which have been incubated in normal BWW ("Control" containing 1.7 mM Ca^{2+} for 1 h; gray bar), and treatments (black bars) which have been incubated in Ca^{2+}-free BWW for 30 min, after which Ca^{2+} was reintroduced in a dose-dependent manner for an additional 30 min. (B) Representative histogram showing fluorescence signals from the treatments shown in (A). $N = 3$ split ejaculates. Significant difference from the control [gray bar; (A)] denoted by $^{**}p \leq 0.01$ and $^{***}p \leq 0.001$.

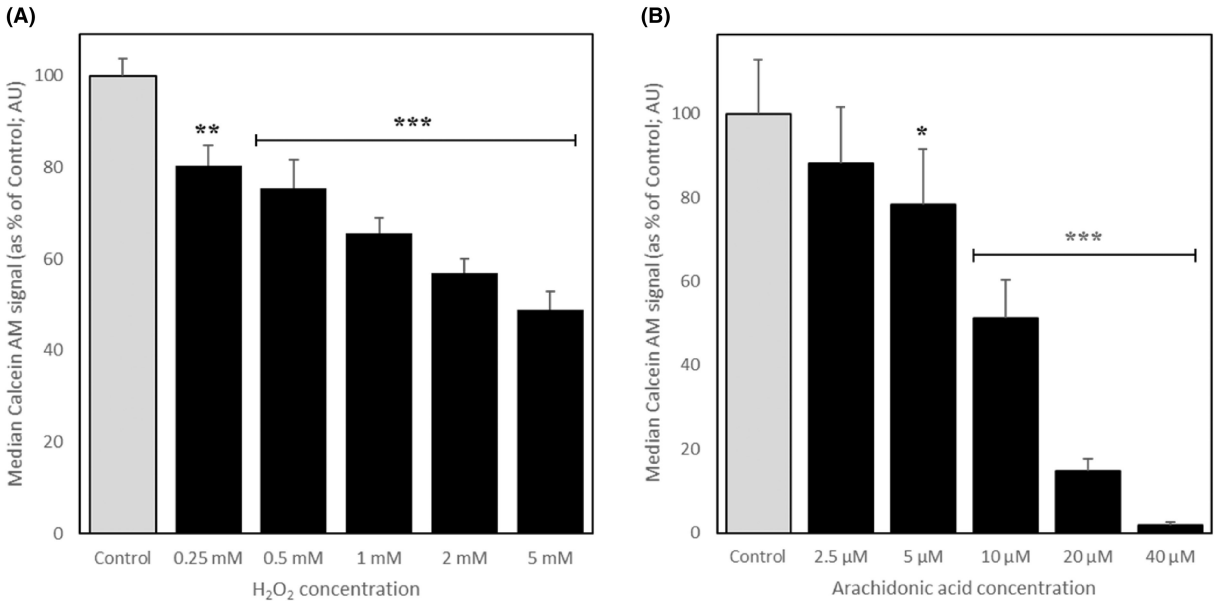

FIGURE 5 Stallion sperm mitochondrial permeability transition pore (mPTP) formation in response to oxidative stress using exogenous [(A) H_2O_2] and endogenous [(B) stimulated by AA] sources of reactive oxygen species. The sperm mPTP formed in response to oxidative stress using physiological doses of AA, but the IC_{50} was achieved only at supraphysiological doses of H_2O_2. $N = 9$ split ejaculates. Significant difference from the control [gray bar; (A)] denoted by $^{*}p \leq 0.05$, $^{**}p \leq 0.01$, and $^{***}p \leq 0.001$. AA, arachidonic acid.

14.8 ± 2.9 AFU, $p \leq 0.001$; 40 µM: 1.8 ± 0.7 AFU, $p \leq 0.001$; Figure 5B) again, indicating a redox-dependent opening of the pore. The concentration of H_2O_2 required to reach the IC_{50} for mPTP formation was in the supraphysiological range, while the dose of AA required to reach the IC_{50} for mPTP formation was well within normal physiological ranges. For this reason, AA was chosen as the instigator of oxidative stress in all succeeding experiments. All fluorescence data were normalized to the control.

3.5 | Experiment 5. Exposure to AA causes an increase in mitochondrial ROS which precedes mPTP formation

Arachidonic acid may stimulate mPTP formation directly,[29] leading us to question whether the results presented in Figure 5B were due to AA-initiated mPTP formation (which then leads to mitochondrial ROS production), or AA-initiated mitochondrial ROS production (which leads to mPTP formation). To ascertain the dynamic relationship between mPTP formation and oxidative stress in response to AA exposure, an AA dose response (0, 2.5, 5, 10, 20, and 40 μM) was conducted for 1 h at 37°C, after which the MSR/mPTP assay was conducted (Section 2.4.5).

The LIVE/DEAD Violet/MSR/C-AM-G triple staining technique revealed that mitochondrial ROS increases prior to the formation of the mPTP when AA is used to instigate oxidative stress (Figure 6). At 2.5 μM AA, the proportion of MSR bright/C-AM-G bright (high ROS but no mPTP formation) spermatozoa was increased compared with the control (5.6 ± 2.2% vs. 67.1 ± 11.9% for control and 2.5 μM AA, respectively; $p \leq 0.05$), though there was no significant shift in any other population. At 10 μM AA, the mPTP began to form, with the proportion of spermatozoa that were MSR bright and C-AM-G dim increasing (0.4 ± 0.1% vs. 25.4 ± 8.7% for control and 10 μM AA, respectively; $p \leq 0.05$). By 40 μM AA, almost the entire population of spermatozoa (96.7 ± 1.5%) were MSR bright and C-AM-G dim (high ROS and mPTP formation; Figure 6).

3.6 | Experiment 6. Intracellular calcium is implicated in the formation of the ROS (AA)-induced mPTP, but ROS are not implicated in the formation of the calcium (ionomycin)-induced mPTP

To investigate the role of mitochondrial ROS in calcium-induced mPTP formation, and the role of calcium in ROS-induced mPTP formation, spermatozoa ($n = 9$, prepared as per Section 2.2) were exposed to increasing doses of ionomycin and AA respectively.

For the ionomycin dose response, spermatozoa were incubated with 0 (control), 5, 10, 20, 40, 80, and 160 nM ionomycin during staining for the Fluo-4 AM/MSR assay (Section 2.4.4). When ionomycin was used to stimulate increased intracellular Ca^{2+}, mPTP formation (loss of C-AM-G brightness) occurred at the same ionomycin dose (40 nM) as that which stimulated a significant intracellular Ca^{2+} increase (Fluo-4 brightness) compared with the control (C-AM-G bright: 82.8 ± 6.9% vs. 22.1 ± 11.4% for control and 40 nM ionomycin, respectively, $p \leq 0.05$; Fluo-4 bright: 2.3 ± 0.6% vs. 51.0 ± 7.7% for control and 40 nM

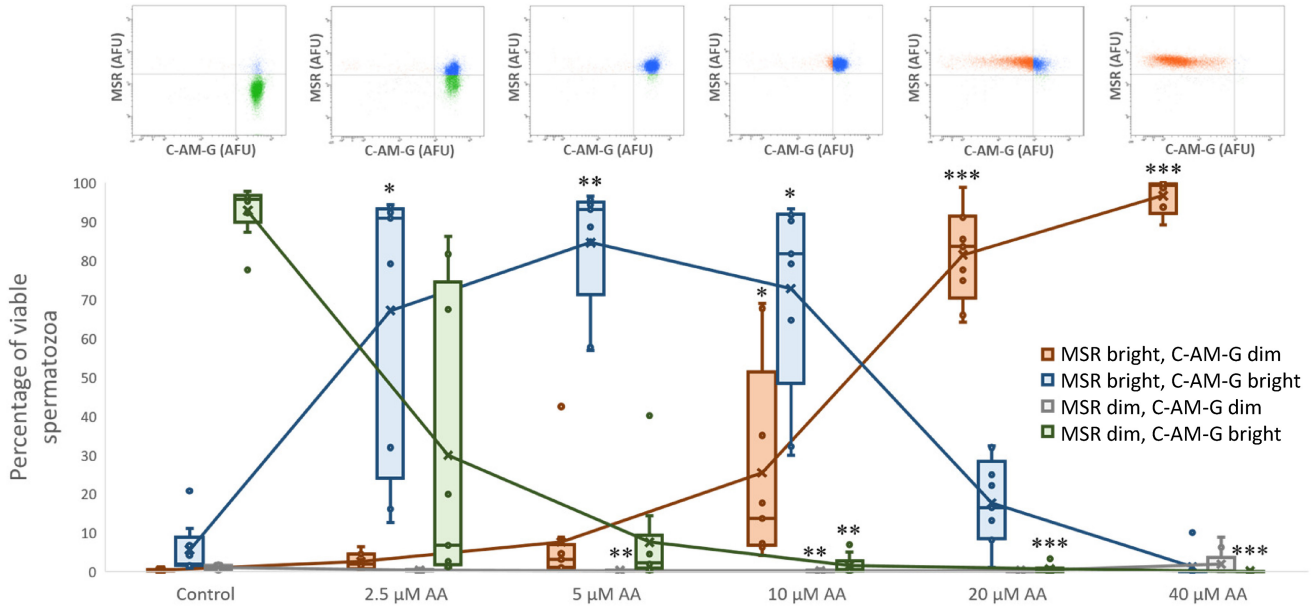

FIGURE 6 Characterizing the dynamic relationship between oxidative stress and mitochondrial permeability transition pore (mPTP) formation. A triple staining technique (LIVE/DEAD Violet to gate viable spermatozoa into a MitoSox Red [MSR] and C-AM-G analysis dot plot) revealed that the mPTP does not begin to form until the cell is in a state of oxidative stress (MSR bright). Each series in the graph (bottom) corresponds to a quadrant from the flow cytometry output (shown in the representative dot plots above each treatment group), denoted by the same color; orange = MSR bright/C-AM-G dim; blue = MSR bright/C-AM-G bright; gray = MSR dim/C-AM-G dim; and green = MSR dim/C-AM-G dim. $N = 9$ split ejaculates. Significant difference from the control (pairwise comparisons using Bonferroni corrections) denoted by *$p \leq 0.05$, **$p \leq 0.01$, and ***$p \leq 0.001$. C-AM-G, calcein AM Green.

ionomycin, respectively, $p \leq 0.01$; Figure 7A), though mitochondrial ROS did not increase until a dose of 160 nM ionomycin (MSR bright: 6.1 ± 2.0% vs. 40.4 ± 8.0% for control and 160 nM ionomycin, respectively, $p \leq 0.001$; Figure 7A).

For the AA dose response, spermatozoa were incubated with 0 (control), 2.5, 5, 10, and 20 μM AA for 45 min at 37°C prior to running the Fluo-4 AM/MSR assay (Section 2.4.4). When AA was used to stimulate mitochondrial ROS production, MSR fluorescence increased at 2.5 μM AA (5.6 ± 1.9% vs. 63.3 ± 11.5% for control and 2.5 μM AA, respectively, $p \leq 0.001$; Figure 7B), but mPTP formation (loss of C-AM-G brightness) did not occur until 10 μM AA (C-AM-G bright: 98.4 ± 0.2% vs. 74.3 ± 3.9% for control and 10 μM AA, respectively, $p \leq 0.05$; Figure 7B). Intracellular Ca^{2+} began to increase at 20 μM AA following mPTP formation (Fluo-4 bright: 2.7 ± 0.6% vs. 40.6 ± 3.6% for control and 20 μM AA respectively, $p \leq 0.001$; Figure 7B).

Given that the mPTP formed in the absence of any source of exogenous Ca^{2+} (Figure 4), as well as under conditions of oxidative stress with no detectable increase in intracellular Ca^{2+} (Figure 7B), we sought to ascertain whether ROS-induced mPTP formation can be mediated by intracellular Ca^{2+} reserves. To ascertain whether intracellular sources of Ca^{2+} might be mediating ROS-induced mPTP formation, spermatozoa ($n = 9$, prepared as per Section 2.2) were divided into two aliquots, one of which was left at RT, and the other was preloaded with 5 μM 1,2-bis(2-aminophenoxy)ethane-*N*,*N*,*N*′,*N*′-tetraacetic acid tetrakis(acetoxymethyl ester) (BAPTA-AM, a powerful membrane permeable Ca^{2+} chelator) for 30 min at 37°C. Each of these aliquots (untreated and BAPTA-AM-preloaded) were then divided again, with one of each receiving no further treatment, and the other being exposed to 20 μM AA for 45 min at 37°C. After this, the C-AM assay (as described in Section 2.4.1) was conducted on all four treatments (Control, BAPTA-AM only, AA only, and BAPTA-AM + AA), with the important distinction that both BAPTA-AM-preloaded treatments (BAPTA-AM only and BAPTA-AM + AA) were resuspended in BWW containing 5 μM BAPTA-AM prior to flow cytometric analyses.

Preloading spermatozoa with BAPTA-AM, a potent Ca^{2+} chelator, prior to the addition of AA to instigate oxidative stress, significantly reduced mPTP formation, such that there was no difference between the median C-AMG fluorescence signals of the control (100 ± 13.0 AFU) and the BAPTA-AM + AA treatment (100 ± 13.0 AFU; Figure 8).

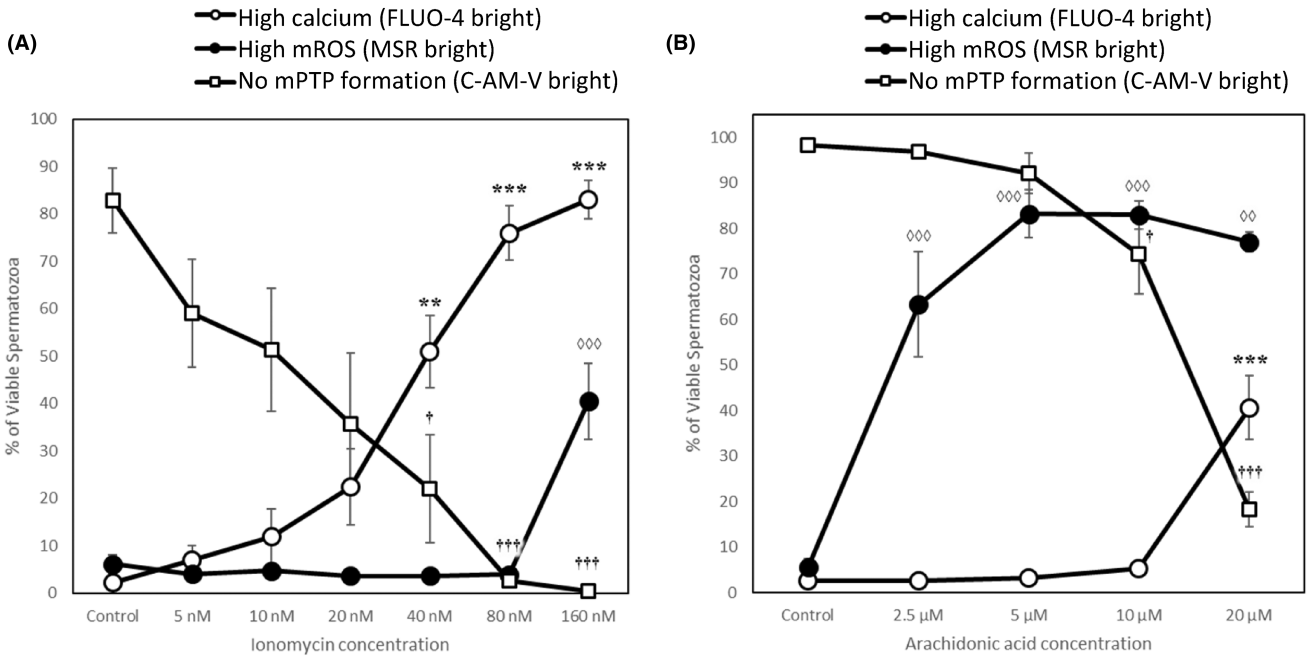

FIGURE 7 The stallion sperm mitochondrial permeability transition pore (mPTP) is more sensitive to increases in calcium [Ca^{2+}; (A)] than increases in ROS (B), though mPTP formation via either mechanism is independent of the other. (A) The mPTP forms (loss of calcein AM Violet [C-AM-V] fluorescence) immediately in response to elevated Ca^{2+} (Fluo-4), both of which become significantly different from the control at 40 nM of ionomycin with no increase in mitochondrial ROS. (B) Mitochondrial ROS increases significantly at 2.5 μM arachidonic acid (AA), which is followed by mPTP formation at doses at or above 10 μM AA, while intracellular Ca^{2+} does not increase until a dose of 20 μM AA. $N = 3$ split ejaculates. Significant difference from the control (Dunnett's test) denoted by "†" ($p \leq 0.05$); "**" or "◊◊" ($p \leq 0.01$); and "***", "◊◊◊" or "†††" ($p \leq 0.001$) for intracellular Ca^{2+} (Fluo-4), mitochondrial ROS (MSR), and mPTP formation (C-AM-V fluorescence loss), respectively. ROS, reactive oxygen species.

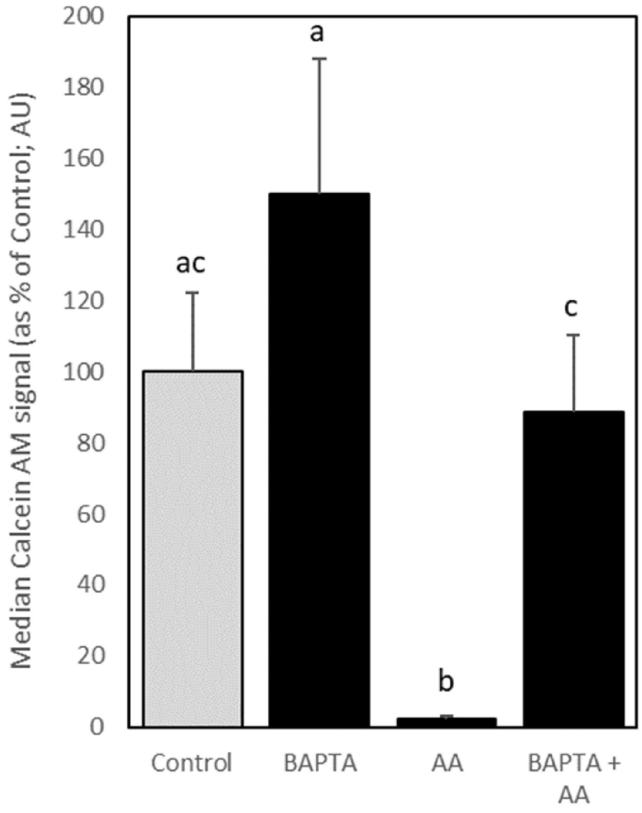

FIGURE 8 BAPTA-AM inhibits stallion sperm mitochondrial permeability transition pore (mPTP) formation in response to oxidative stress stimulated by arachidonic acid (AA). Formation of the sperm mPTP in response to 20 μM AA can be inhibited via pretreatment with BAPTA-AM (5 μM), suggesting that reactive oxygen species-induced mPTP formation is mediated by intracellular Ca^{2+}. $N = 10$ split ejaculates. Significant difference from the control (gray bar) denoted by different letter superscripts ($p \leq 0.05$). BAPTA-AM, 1,2-bis(2-aminophenoxy)ethane-*N*,*N*,*N*′,*N*′-tetraacetic acid tetrakis(acetoxymethyl ester).

4 | DISCUSSION

This is the first study to examine the phenomenon of mPTP formation in stallion spermatozoa and to characterize the events surrounding mPTP formation in this cell type. We hypothesized that the stallion sperm mPTP plays a vital role in the maintenance of calcium and ROS homeostasis and that the C-AM assay will provide the most sensitive measure of mPTP formation. Indeed, our results showed that the mPTP forms in stallion spermatozoa following both oxidative stress and intracellular Ca^{2+} perturbation, and that these mechanisms both rely on intracellular Ca^{2+} reserves to modulate mPTP formation. Importantly, the formation of the mPTP is not synonymous with mitochondrial membrane depolarization and is not always detrimental to sperm function and survival.

The formation of the mPTP refers to a phenomenon whereby the inner mitochondrial membrane becomes permeable to ions and solutes of less than 1500 Da in size. While the structure of this ion channel remains unresolved, it is generally accepted that the defining features of the mPTP are that it forms in response to elevated levels of Ca^{2+}, and that CyPD is somehow involved in this process by virtue of mPTP formation being inhibited by CsA (a binder of CyPD).[29,30] It is commonly assumed that mPTP formation causes a loss of MMP, resulting in a rapid impairment of mitochondrial function and swelling of the mitochondria, ending in cell death.[31] Close associations between MMP loss and mPTP formation have been reported in neurons,[32] and previous studies have equated a loss of MMP with mPTP formation in several cell types,[33] including spermatozoa.[17,23] In the present study, we set out to establish whether such a close association between mPTP formation and MMP depolarization existed in stallion spermatozoa, by simultaneously examining mitochondrial membrane status using JC-1, and mPTP formation using a loss of C-AM-V fluorescence. Our results demonstrate that in this cell type, a loss of MMP does not necessarily coincide with mPTP formation (Figure 1); indeed, one of the gating controls for the JC-1/C-AM-V assay used in the present study is CCCP, which collapsed MMP without any loss of C-AM-V fluorescence (and therefore no mPTP formation; Figure 1C), demonstrating that a loss of MMP may be due to reasons other than mPTP formation. However, prolonged mPTP formation does eventually lead to MMP loss (Figure 2B). There are several implications of this observation; first, by equating the two assays, MMP loss is incorrectly used to diagnose mPTP formation, and the downstream effects of MMP loss (which are predominantly deleterious) are then attributed to mPTP formation. As a result, mPTP formation is demonized as part of the apoptotic process, and efforts are made to inhibit the process. Based upon the findings of the present study, the fact that mPTP formation does not always result in MMP loss led us to suppose that mPTP formation in stallion spermatozoa may play a homeostatic—rather than exclusively pathological—role in the mitochondria of these cells, in which case inhibition would be contraindicated.

Despite the longstanding debate about mPTP structure, one particular feature that is generally agreed upon is an absolute specificity for Ca^{2+} and inhibition by CsA, a CyPD inhibitor, the use of which has been shown to desensitize the mPTP to the effects of elevated calcium, at least in the case of somatic cells.[9] In order to fairly evaluate the ability of CsA to inhibit mPTP formation in this cell type, we needed to establish the minimum dose of the Ca^{2+} ionophore, ionomycin, required to achieve the IC_{50} for mPTP formation. Interestingly, we found that the IC_{50} was as low as 10 nM ionomycin (Figure 3A), which is 100× lower than the standard concentration

utilized for the majority of studies, and 100× lower than the negative control treatment for the commercial calcein AM/$CoCl_2$ assay kit (MitoProbe™). For this reason, we utilized 10 nM ionomycin for all subsequent experiments. Different cell types exhibit various degrees of responsiveness to CsA-inhibition of mPTP formation,[29] and limited prior studies suggest that mammalian spermatozoa are particularly resistant to mPTP inhibition by CsA.[19] Similarly, our study has shown that CsA is not effective in preventing mPTP formation in stallion sperm mitochondria (Figure 3B). As such, it appears that this cell type does not form the "classical" mPTP, in that mPTP formation can be induced by Ca^{2+} ionophore but cannot be inhibited by CsA. Because CsA is a specific inhibitor of CyPD, this implies that CyPD is not involved in mPTP formation in spermatozoa. The reasons for this difference are unclear, but it has been suggested that reduced CyPD activity may confer cells with enhanced resistance to Ca^{2+}-induced mPTP formation.[34] Whether mammalian spermatozoa are indeed less sensitive to Ca^{2+} fluctuations than somatic cells remains to be determined. However, it is conceivable that mammalian spermatozoa, which rely on the entry of Ca^{2+} into the cell via CatSper channels (sperm-specific calcium channels) to facilitate capacitation,[35] may have evolved to reduce susceptibility to Ca^{2+}-induced mPTP formation by downregulating their expression of CyPD. This idea finds support in the fact that sea urchin spermatozoa, unlike mammalian spermatozoa, *are* susceptible to CsA inhibition of mPTP formation.[23] In sea urchins, the capacitation-like process ("activation") triggered during spawning does not depend on Ca^{2+} but instead results from an increase in intracellular pH. Substantial increases in Ca_i^{2+} occur only when the sperm encounters the egg's jelly coat, leading to the acrosome reaction and the rapid death of the spermatozoon if fertilization does not occur.[36] Therefore, in this aquatic species, tolerance to high Ca_i^{2+} may not be necessary as it is in mammalian spermatozoa.

Exposure to excess calcium is one of the major triggers for mPTP formation and implicates the mitochondrial pore system in initiation of apoptosis. More recently, it has been demonstrated that other stimuli, such as oxidative stress, can also trigger mPTP formation,[7,20] but whether the path from ROS-induced mPTP formation to apoptosis is still mediated through exogenous Ca^{2+} uptake remains unclear, as oxidative states are often concurrent with cytosolic and mitochondrial Ca^{2+} influx.[37] In characterizing the mPTP in stallion spermatozoa, we sought to determine whether the presence of exogenous Ca^{2+} was an essential requirement for pore formation. Interestingly, we found not only that the stallion sperm mPTP is not reliant on an exogenous source of Ca^{2+} (Figure 3C) but also that the mPTP rapidly forms when deprived of Ca^{2+}, perhaps in an effort to allow Ca^{2+} to flow into the mitochondria for the maintenance of intracellular Ca^{2+} homeostasis. This hypothesis was supported by our observation that mPTP formation in a Ca^{2+}-free medium was reversed with the addition of Ca^{2+} to the medium in a dose-dependent manner (Figure 4). This is the first study to show that mPTP formation does not require extracellular Ca^{2+} and also the first to demonstrate a role for mPTP in Ca^{2+} homeostasis in stallion spermatozoa.

There are conflicting opinions regarding the relationship between mPTP formation and ROS production; some postulate that the mPTP forms in response to elevated ROS,[7,20] while others suggest that elevated ROS are the result of mPTP formation.[19,38] Thus, we next sought to determine whether ROS could serve as a trigger for mPTP formation in spermatozoa, and thereby clarify the sequence of events: do ROS lead to mPTP formation, or does mPTP formation lead to ROS production? An important consideration in answering this question is whether the oxidative state is the result of endogenous ROS production within the cell or the addition of exogenous ROS. While other studies have used the addition of H_2O_2 to stimulate ROS-induced mPTP formation, in this study we found that the mPTP IC_{50} was met only at supraphysiological H_2O_2 concentrations (Figure 5A), making it unsuitable as a model of in vivo mPTP formation in this cell type. Previous work from this group and others has revealed that AA is a powerful instigator of mitochondrial ROS production in spermatozoa,[27,28] the most likely mechanism for this being the inhibition of specific mitochondrial electron transport chain (ETC) complexes by the unsaturated fatty acid, causing electron leakage and subsequent formation of superoxide.[39] Additional reasons for selecting AA for this purpose are that it has previously been shown to stimulate mitochondrial ROS production in a highly significant and dose-dependent manner, even at physiological levels as low as 6.25 μM.[40] A brief exposure to AA does not adversely affect sperm motility or vitality in the short term but can sustain oxidative stress over an extended period, as evidenced by its significant impact on oxidative DNA damage,[40] further underscoring its suitability as a ROS inducer in the present study.

In our experiments, treatment with AA rapidly induced mPTP formation in spermatozoa at physiologically relevant concentrations (Figure 5B). However, it must be noted that there is another mechanism through which AA could have led to mPTP formation; AA can mimic the effects of TNF-α,[41] which triggers activation of pro-apoptotic events, including prolonged mPTP opening.[13] To confirm that AA-induced mPTP formation was indeed mediated via endogenous ROS production in the present study, we

further examined the dynamic relationship between actual sperm oxidative stress and mPTP formation in response to increasing concentrations of AA (Figure 6). These experiments revealed that as the concentration of AA increases, the mPTP does not begin to form until the cell is in a state of oxidative stress (MitoSox Red bright), suggesting that mPTP formation in response to AA is indeed mediated via an oxidative stress mechanism. However, to confirm this hypothesis, it would be necessary to investigate whether apoptotic markers are also activated in response to AA exposure.

Treulen et al.[19] have suggested that mPTP formation in mammalian spermatozoa leads to the production of ROS, and under certain conditions, such as high intracellular Ca^{2+}, we also found this to be the case, where ionomycin-triggered mPTP formation eventually led to elevated mitochondrial ROS production, as measured by the MitoSox Red probe (Figure 7A). Indeed, the relationship between mPTP formation, calcium, and ROS is a complex one, but the results of the present study show that endogenous ROS stimulate mPTP formation (Figure 7B) via an intracellular Ca^{2+}-dependent mechanism (Figure 8), and that elevated Ca^{2+} stimulates mPTP formation via a ROS-independent mechanism (Figure 7A). Furthermore, mPTP formation via either stimulus results in the downstream elevation of the other (Figure 7). It should be noted that following ROS-induced mPTP formation, it was not until the mPTP had completely formed that we observed an increase in intracellular calcium using the Fluo-4 probe (Figure 7B), which suggested that ROS-induced mPTP formation may be a Ca^{2+} independent event; a hypothesis that has previously been proposed.[33] However, by chelating intracellular Ca^{2+} using BAPTA-AM, we were able to inhibit ROS-induced mPTP formation (Figure 8), confirming that the stallion sperm mPTP is indeed mediated by Ca^{2+}, although at undetectable concentrations. The increase in ROS following Ca^{2+}-stimulated mPTP formation may also be due to the activation of NADPH oxidases (NOXs), which produce ROS (superoxide and hydrogen peroxide) that interfere with ETC function.[42] Indeed, the major NOX species in stallion spermatozoa is NOX5 which is known to generate ROS in a calcium-dependent manner.[43] Furthermore, exogenous AA may directly or indirectly perturb the ETC (via NOX activation), with ETC perturbation leading to increased leakage of superoxide and exacerbation of the oxidative stress cascade.[44,45]

A major limitation of this study is the reliance on a single method for measuring mPTP formation—the C-AM assay. This limitation stems from the current lack of alternative assays capable of detecting the *early* stages of mPTP formation, as opposed to measurable downstream events like mitochondrial swelling or cytochrome c release. Although the prospects of fluorescence resonance energy transfer-based assays or proximity ligation assays were considered, our incomplete understanding of the proteins involved in mPTP formation, especially in spermatozoa, presents a barrier to confidently targeting specific proteins for these assays.

In conclusion, the stallion spermatozoon does not form the "classical" mPTP; it is not sensitive to inhibition by CsA, and while it is not dependent on an exogenous source of Ca^{2+}, it appears that intracellular Ca^{2+} stores are sufficient to mediate this process. Furthermore, mPTP formation is not closely coupled with a loss of MMP, and for this reason, it is not appropriate to use the JC-1 assay as a proxy for the C-AM assay. In these cells, the mPTP forms in response to elevated endogenous ROS, or $[Ca^{2+}]$ outside normal physiological ranges, where it plays a vital role in the maintenance of homeostasis. As such, care should be taken when using mPTP inhibitors to improve in vitro sperm longevity.[23,46] Certainly, in the horse, it is more appropriate to address the events upstream of mPTP formation, such as Ca^{2+} or ROS imbalance, which lead to and are somewhat ameliorated by mPTP formation.

AUTHOR CONTRIBUTIONS

Zamira Gibb co-conceived the idea for the manuscript, conducted most of the experimental work and statistical analyses, and wrote the manuscript. Robert J. Aitken and Aleona Swegen co-conceived the idea for the manuscript and contributed to experimental design. Alecia R. Sheridan, Brandan Holt, and Stephanie Waugh all contributed to experimental design and conducted/optimized several of the experiments described in this manuscript. All authors were involved in drafting and revising the manuscript.

ACKNOWLEDGMENTS

The authors acknowledge the University of Newcastle's Analytical and Biomolecular Research Facility for providing the use and maintenance of the flow cytometer. Open access publishing facilitated by The University of Newcastle, as part of the Wiley - The University of Newcastle agreement via the Council of Australian University Librarians.

FUNDING INFORMATION

The authors thank the Australian Research Council, which provided grant funding to support this research (DECRA Fellowship: DE180100894 and Future Fellowship: FT220100557).

DISCLOSURES

The authors declare no conflict of interest.

DATA AVAILABILITY STATEMENT

The data set for the present study is available as a Supporting Information to this manuscript.

ORCID

Zamira Gibb https://orcid.org/0000-0002-4864-8880
Robert J. Aitken https://orcid.org/0000-0002-9152-156X
Alecia R. Sheridan https://orcid.org/0009-0006-3814-9734
Brandan Holt https://orcid.org/0009-0001-2560-085X
Stephanie Waugh https://orcid.org/0000-0002-2125-2288
Aleona Swegen https://orcid.org/0000-0001-7371-5400

REFERENCES

1. Aitken RJ, Curry BJ. Redox regulation of human sperm function: from the physiological control of sperm capacitation to the etiology of infertility and DNA damage in the germ line. *Antioxid Redox Signal*. 2011;14:367-381.
2. Gibb Z, Lambourne SR, Curry BJ, Hall SE, Aitken RJ. Aldehyde dehydrogenase plays a pivotal role in the maintenance of stallion sperm motility. *Biol Reprod*. 2016;94(6):1-11.
3. White IG. Lipids and calcium uptake of sperm in relation to cold shock and preservation: a review. *Reprod Fertil Dev*. 1993;5:639-658.
4. Gibb Z, Holt B, Swegen A, Lambourne SR, Aitken RJ. Mitochondrial permeability transition pore formation during chilling and cryopreservation of stallion spermatozoa. Paper Presented at: 48th Annual Scientific Meeting of the Endocrine Society of Australia and the Society for Reproductive Biology; August 27–30, 2017; Perth, Australia.
5. Stewart TA, Davis FM. An element for development: calcium signaling in mammalian reproduction and development. *Biochim Biophys Acta Mol Cell Res*. 2019;1866:1230-1238.
6. Guthrie HD, Welch GR, Woods LC. Effects of frozen and liquid hypothermic storage and extender type on calcium homeostasis in relation to viability and ATP content in striped bass (*Morone saxatilis*) sperm. *Theriogenology*. 2014;81:1085-1091.
7. Panel M, Ghaleb B, Morin D. Mitochondria and aging: a role for the mitochondrial transition pore? *Aging Cell*. 2018;17:e12793.
8. Hunter DR, Haworth RA. The Ca^{2+}-induced membrane transition in mitochondria: I. The protective mechanisms. *Arch Biochem Biophys*. 1979;195:453-459.
9. Leung AWC, Varanyuwatana P, Halestrap AP. The mitochondrial phosphate carrier interacts with cyclophilin D and may play a key role in the permeability transition. *J Biol Chem*. 2008;283:26312-26323.
10. Giorgio V, von Stockum S, Antoniel M, et al. Dimers of mitochondrial ATP synthase form the permeability transition pore. *Proc Natl Acad Sci U S A*. 2013;110:5887-5892.
11. Bonora M, Morganti C, Morciano G, et al. Mitochondrial permeability transition involves dissociation of F_1F_O ATP synthase dimers and C-ring conformation. *EMBO Rep*. 2017;18:1077-1089.
12. Baines CP, Gutierrez-Aguilar M. The still uncertain identity of the channel-forming unit(s) of the mitochondrial permeability transition pore. *Cell Calcium*. 2018;73:121-130.
13. Soriano ME, Nicolosi L, Bernardi P. Desensitization of the permeability transition pore by cyclosporin a prevents activation of the mitochondrial apoptotic pathway and liver damage by tumor necrosis factor-alpha. *J Biol Chem*. 2004;279:36803-36808.
14. Akopova OV, Kolchinskaya LI, Nosar VI, Bouryi VA, Mankovska IN, Sagach VF. Cytochrome C as an amplifier of ROS release in mitochondria. *Fiziol Zh (1994)*. 2012;58:3-12.
15. Wu L, Liu X, Cao KX, Ni Z, Li WD, Chen ZP. Synergistic antitumor effects of rhein and doxorubicin in hepatocellular carcinoma cells. *J Cell Biochem*. 2020;121:4009-4021.
16. Wang H, Dou S, Zhu J, et al. Ghrelin protects against rotenone-induced cytotoxicity: involvement of mitophagy and the AMPK/SIRT1/PGC1α pathway. *Neuropeptides*. 2021;87:102134.
17. Ferrusola CO, Fernández LG, Sandoval CS, et al. Inhibition of the mitochondrial permeability transition pore reduces "apoptosis like" changes during cryopreservation of stallion spermatozoa. *Theriogenology*. 2010;74:458-465.
18. Petronilli V, Miotto G, Canton M, Colonna R, Bernardi P, Di Lisa F. Imaging the mitochondrial permeability transition pore in intact cells. *Biofactors*. 1998;8:263-272.
19. Treulen F, Uribe P, Boguen R, Villegas JV. Mitochondrial permeability transition increases reactive oxygen species production and induces DNA fragmentation in human spermatozoa. *Hum Reprod*. 2015;30:767-776.
20. Fang Y, Zhao C, Xiang H, Zhao X, Zhong R. Melatonin inhibits formation of mitochondrial permeability transition pores and improves oxidative phosphorylation of frozen-thawed ram sperm. *Front Endocrinol (Lausanne)*. 2019;10:896.
21. Huang J, Zhong Y, Fang X, et al. Hepatitis B virus S protein enhances sperm apoptosis and reduces sperm fertilizing capacity in vitro. *PLoS One*. 2013;8:e68688.
22. Treulen F, Arias ME, Aguila L, Uribe P, Felmer R. Cryopreservation induces mitochondrial permeability transition in a bovine sperm model. *Cryobiology*. 2018;83:65-74.
23. Torrezan-Nitao E, Boni R, Marques-Santos LF. Mitochondrial permeability transition pore (MPTP) desensitization increases sea urchin spermatozoa fertilization rate. *Cell Biol Int*. 2016;40:1071-1083.
24. Gibb Z, Lambourne SR, Aitken RJ. The paradoxical relationship between stallion fertility and oxidative stress. *Biol Reprod*. 2014;91(3):1-10.
25. Plaza Davila M, Martin Munoz P, Tapia JA, Ortega Ferrusola C, Balao da Silva CC, Pena FJ. Inhibition of mitochondrial complex I leads to decreased motility and membrane integrity related to increased hydrogen peroxide and reduced ATP production, while the inhibition of glycolysis has less impact on sperm motility. *PLoS One*. 2015;10:e0138777.
26. Biggers JD, Whitten WK, Whittingham DG. The culture of mouse embryos in vitro. In: Daniels JC, ed. *Methods in Mammalian Embryology*. Freeman; 1971:86-116.
27. Aitken RJ, Wingate JK, De Iuliis GN, Koppers AJ, McLaughlin EA. Cis-unsaturated fatty acids stimulate reactive oxygen species generation and lipid peroxidation in human spermatozoa. *J Clin Endocrinol Metab*. 2006;91:4154-4163.
28. Koppers AJ, Garg ML, Aitken RJ. Stimulation of mitochondrial reactive oxygen species production by unesterified, unsaturated fatty acids in defective human spermatozoa. *Free Radic Biol Med*. 2010;48:112-119.

29. Di Paola M, Zaccagnino P, Oliveros-Celis C, Lorusso M. Arachidonic acid induces specific membrane permeability increase in heart mitochondria. *FEBS Lett*. 2006;580:775-781.
30. Carroll J, He J, Ding S, Fearnley IM, Walker JE. Persistence of the permeability transition pore in human mitochondria devoid of an assembled ATP synthase. *Proc Natl Acad Sci U S A*. 2019;116:12816-12821.
31. Lefer DJ, Bolli R. Chapter 28 – Cardioprotection. In: Hill JA, Olson EN, eds. *Muscle. Fundamental Biology and Mechanisms of Disease*. Academic Press; 2012:369-388.
32. Arrázola MS, Ramos-Fernández E, Cisternas P, Ordenes D, Inestrosa NC. Wnt signaling prevents the Aβ oligomer-induced mitochondrial permeability transition pore opening preserving mitochondrial structure in hippocampal neurons. *PLoS One*. 2017;12:e0168840.
33. Maia RC, Culver CA, Laster SM. Evidence against calcium as a mediator of mitochondrial dysfunction during apoptosis induced by arachidonic acid and other free fatty acids. *J Immunol*. 2006;177:6398-6404.
34. Sartori MR, Navarro CDC, Castilho RF, Vercesi AE. Enhanced resistance to Ca^{2+}-induced mitochondrial permeability transition in the long-lived red-footed tortoise *Chelonoidis carbonaria*. *J Exp Biol*. 2022;225:jeb243532.
35. Hwang JY, Chung J-J. CatSper calcium channels: 20 years on. *Phys Ther*. 2023;38:125-140.
36. Shapiro BM, Cook S, Quest AF, Oberdorf J, Wothe D. Molecular mechanisms of sea-urchin sperm activation before fertilization. *J Reprod Fertil Suppl*. 1990;42:3-8.
37. Ermak G, Davies KJ. Calcium and oxidative stress: from cell signaling to cell death. *Mol Immunol*. 2002;38:713-721.
38. Song X, Zhang L, Hui X, et al. Selenium-containing protein from selenium-enriched *Spirulina platensis* antagonizes oxygen glucose deprivation-induced neurotoxicity by inhibiting ROS-mediated oxidative damage through regulating MPTP opening. *Pharm Biol*. 2021;59:629-638.
39. Cocco T, Di Paola M, Papa S, Lorusso M. Arachidonic acid interaction with the mitochondrial electron transport chain promotes reactive oxygen species generation. *Free Radic Biol Med*. 1999;27:51-59.
40. Aitken RJ, Smith TB, Lord T, et al. On methods for the detection of reactive oxygen species generation by human spermatozoa: analysis of the cellular responses to catechol oestrogen, lipid aldehyde, menadione and arachidonic acid. *Andrology*. 2013;1:192-205.
41. Scorrano L, Penzo D, Petronilli V, Pagano F, Bernardi P. Arachidonic acid causes cell death through the mitochondrial permeability transition. Implications for tumor necrosis factor-α apoptotic signaling. *J Biol Chem*. 2001;276:12035-12040.
42. Görlach A, Bertram K, Hudecova S, Krizanova O. Calcium and ROS: a mutual interplay. *Redox Biol*. 2015;6:260-271.
43. Sabeur K, Ball BA. Characterization of NADPH oxidase 5 in equine testis and spermatozoa. *Reproduction*. 2007;134:263-270.
44. Aitken RJ, Whiting S, De Iuliis GN, McClymont S, Mitchell LA, Baker MA. Electrophilic aldehydes generated by sperm metabolism activate mitochondrial reactive oxygen species generation and apoptosis by targeting succinate dehydrogenase. *J Biol Chem*. 2012;287:33048-33060.
45. Aitken RJ, Gibb Z, Mitchell LA, Lambourne SR, Connaughton HS, De Iuliis GN. Sperm motility is lost in vitro as a consequence of mitochondrial free radical production and the generation of electrophilic aldehydes but can be significantly rescued by the presence of nucleophilic thiols. *Biol Reprod*. 2012;87(5):1-11.
46. Fang Y, Zhao C, Xiang H, Jia G, Zhong R. Melatonin improves cryopreservation of ram sperm by inhibiting mitochondrial permeability transition pore opening. *Reprod Domest Anim*. 2020;55:1240-1249.

SUPPORTING INFORMATION

Additional supporting information can be found online in the Supporting Information section at the end of this article.

How to cite this article: Gibb Z, Aitken RJ, Sheridan AR, Holt B, Waugh S, Swegen A. The effects of oxidative stress and intracellular calcium on mitochondrial permeability transition pore formation in equine spermatozoa. *FASEB BioAdvances*. 2024;6:143-158. doi:10.1096/fba.2023-00051